Characteristics of $Co_xTi_{1-x}O_2$ Thin Films Deposited by MOCVD

Adam McClure[a)], A. Kayani, and Y. U. Idzerda

Department of Physics, Montana State University, Bozeman, Montana 59717

E. Arenholz and E. Cruz

Advanced Light Source, Lawrence Berkeley National Laboratory, Berkeley, California 94720

Abstract

This paper deals with the growth and characterization of ferromagnetic cobalt doped TiO_2 thin films deposited by liquid precursor metal organic chemical vapor deposition (MOCVD) using a new combination of the source materials $Co(TMHD)_3$, tetrahydrofuran (THF), and titanium isopropoxide (TIP). An array of experiments reveals the intrinsic ferromagnetic nature of the grown films, and suggests that the magnetism is not generated by oxygen vacancies.

[a)] Electronic mail: mcclure@physics.montana.edu

I. Introduction

There is a growing recognition of the uniqueness and value of the novel electronic, magnetic, and optical responses of oxides in the context of modern device applications. As the limits of conventional charge transport electronics are being approached, innovative new concepts will need to be explored to help overcome these limitations. One such concept is the exploitation of the spin of the electron, in addition to its charge, to create a new class of spin transport electronic (spintronic) devices whose impact in the world of microelectronics is already being felt [1,2]. Dilute magnetic semiconductors (DMS), a functional material that is magnetized by introducing local magnetic moments into the host, offer the advantages of the spin degree of freedom and compatibility with existing semiconductor technologies [3].

Cobalt doped semiconducting oxides are of the new generation for DMS. Cobalt doped TiO_2 was the first to exhibit ferromagnetism at room temperature [4]. Since then it has been extensively studied [5,6,7], and other oxides are being explored as potential DMS candidates [8,9]. Ongoing efforts are underway to successfully synthesize, characterize, and understand the properties of these dilute magnetic semiconductors.

One important aspect of this exciting class of materials is that they can be produced in a manner compatible with the fabrication of complex oxide/silicon integrated devices. This requires films with precisely controlled thickness and uniformity, easy variability in doping levels, an ability to deposit films conformally onto three-dimensional structures, and a growth method that it is readily scalable to large area substrates and to industrial production. These demands can be met using metal organic chemical vapor deposition (MOCVD) [10].

II. Experimental

Cobalt doped TiO_2 thin films were prepared using liquid precursor MOCVD. The chemical and structural properties of these films were studied using X-ray absorption spectroscopy (XAS), while the concentrations of the elements and thicknesses of the films were determined by Rutherford backscattering spectrometry (RBS). A vibrating sample magnetometer (VSM) was used to measure the magnetic properties of the films, and annealing studies and X-ray magnetic circular dichroism (XMCD) probed the origins of the magnetism in these DMS materials.

A new combination of precursors was used to make the $Ti_{1-x}Co_xO_2$ thin films. Following from the work done by Seong et al. [11], we used Titanium Isopropoxide $Ti(C_3H_7O)_4$ (TIP), $Co(TMHD)_3$ [TMHD – $C_{11}H_{19}O_2$], and Tetrahydrofuran C_4H_8O (THF) as the liquid precursor. The $Co(TMHD)_3$ powder was first dissolved in THF and then added to the TIP to form a solution that had a Ti to Co ratio of 10:1. This mixture was used to deposit the $Ti_{1-x}Co_xO_2$ thin films on SiO_2/Si, A-plane and R-plane Al_2O_3, and yttria (9%) stabilized zirconia (100) substrates at a temperature range of 300 – 500 °C. The films were around 800 nm thick after 30 minutes of growth, with a Co concentration of 0.5% (x = .005) as determined by RBS using a silicon surface barrier detector in a high vacuum chamber connected to a 2 MeV Van de Graff positive ion accelerator.

The vapor pressure of the liquid precursor was controlled by maintaining its temperature at –5 °C in a Cole-Parmer refrigerated circulating bath. Ultra high purity He was used as a carrier gas to transport the precursor material as a vapor to the hot wall reactor through heated lines held at 60 °C to prevent any condensation of the precursor.

The He flow rate was 45 standard cubic œntimeters per minute (sccm), and oxygen was fed into the reactor at 75 sccm. The flow rates were independently regulated with mass flow controllers. Our system is used for reaction limited types of growths, and the pressure during deposition is about 1 Torr. An 800 1/sec turbomolecular pump is used to regulate the vacuum in the chamber during growth, using a mostly closed butterfly valve to maintain the large pressure differential between the reaction chamber and the turbomolecular pump. To maintain high purity in the gas manifolds when not in use, the transfer lines from the bubblers to the reaction chamber are held under high vacuum by a second 100 1/sec turbomolecular pump.

To determine the effects of annealing on the Co-doped TiO_2 thin films, a subset of identical films was slowly heated to 700 ^oC in an ex-situ gas flow furnace over a 45 minute period, annealed for 2 hours at that temperature, then allowed to slowly cool to room temperature. Anneals were conducted in air, or with an overpressure of flowing He, N_2, or O_2.

III. Results and Discussion

Figure 1 demonstrates the versatility of the MOCVD process to controllably produce either the anatase or rutile structure of the TiO_2 host. The Ti $2p$ ($L_{2,3}$) X-ray absorption spectra (XAS) is a sensitive indicator of these chemically identical structures. In XAS, an absorbed photon promotes a core electron to unoccupied states. The $2p$ XAS spectrum is dominated by electric dipole allowed transitions to the 3d final states. The Ti $2p$ XAS spectra of anatase and rutile TiO_2 have been interpreted as atomic multiplets of $2p^6 3d^0$? $2p^5 3d^1$ transitions projected in a crystal field corresponding to, respectively,

D_{2d} and D_{2h} point group symmetries [12,13]. The spectra shown in Figure 1 can be explained as follows: The $2p$ core-hole spin orbit interaction splits the spectrum into two parts, corresponding to transitions from the $2p_{3/2}$ (L_3-edge) and $2p_{1/2}$ (L_2-edge) levels. The L_2-edge is essentially a duplicate of the L_3-edge, but with the details washed out due to an intrinsic broadening related to core-hole lifetime effects arising from Coster-Kronig Auger decay processes [13,14]. The lowering of symmetry from spherical to octahedral introduces a crystal field responsible for the splitting of each edge into lower energy, more easily accessible, p-bonded t_{2g} antibonding states and higher energy s-bonded e_g antibonding states. The largest differences between the Ti $2p$ XAS spectra of anatase and rutile can be seen in the L_3-edge e_g region. This splitting and asymmetry of the e_g peak is related to the lowering of crystal field symmetry from octahedral (O_h) to D_{2d} and D_{2h} [14]. For the anatase structure (D_{2d}), the spectral weight is shifted to the lower energy peak (left most peak of the doublet), whereas for the rutile structure (D_{2h}) the spectral weight of the doublet is more in the higher energy peak (right most peak). Mixed phase materials (and the brookite phase) have the spectral weight more equally shared between the two peaks. The first two small peaks arise from a forbidden (higher order than electric dipole) transition [12,14].

The XAS spectra reported here were acquired at beamlines 6.3.1 and 4.0.2 of the Advanced Light Source at Lawrence Berkeley National Laboratories. As can be seen from the XAS spectra of the Ti $L_{2,3}$-edge in Figure 1, the anatase phase of TiO_2 is stabilized on Si substrates at lower temperatures, and the thermodynamically favored rutile structure forms at higher temperatures [15]. However, when deposited on A-plane Al_2O_3 single crystal substrates, the rutile structure is preferred for all substrate growth

temperatures. This preference of phase also depends systematically on the oxygen flow-rate during growth, with higher oxygen flow-rates resulting in a more single phase anatase film (as depicted in Figure 2).

The XAS was also used to determine whether the Co is in a substitutional site (for Ti) or an interstitial site in the TiO_2 lattice. Figure 3 shows a comparison of Co $L_{2,3}$-edge XAS spectra for MOCVD deposited Co:TiO_2 thin films and those deposited by pulse laser deposition. The spectra are nearly identical, and this has been shown to be consistent with the cobalt dopants incorporating substitutionally at the Ti sites [16].

In addition to the chemical and structural characteristics of these films, we have also confirmed their magnetic properties. As shown in Figure 4, our as-grown samples show room temperature ferromagnetism as determined by vibrating sample magnetometry. Although the saturation moments of the samples varied, they typically showed 30-35% remnance with a coercive field of about 200 Oe. These results are consistent with other works [16,17], and further confirm that these samples deposited by MOCVD are identical to those synthesized by other methods. Figure 4 also shows another important result: the disappearance of ferromagnetism upon annealing. Annealing the samples at 700 °C for 2 hours in flowing He, N_2, O_2, or air all resulted in the vanishing of the ferromagnetism. These results confirm that oxygen vacancies are not essential for ferromagnetism in the cobalt doped TiO_2 oxide DMS system.

Finally, to determine the nature of the ferromagnetism in these materials, we used X-ray magnetic circular dichroism (XMCD) on the Co $L_{2,3}$-edges. XMCD is an element specific technique with strong magnetic contrast that has been successfully employed to measure induced magnetic moments [18], identify element specific magnetic ordering

[19], acquire element specific magnetic hysteresis loops [20], and determine individually the orbital [21] and spin [22] contributions to the overall moment of an element [23].

In this technique, two XAS spectra are alternatively obtained using circularly polarized light, with the magnetization direction of the sample reversed at each photon energy. The use of circularly polarized light and reversed magnetization preferentially promote transitions of either up-spin or down-spin electrons to the Fermi level. Because a ferromagnet has more unfilled states at the Fermi level for one electron spin orientation, the absorption is enhanced for the corresponding magnetization direction. The XMCD intensity is obtained by computing the difference between the two spectra. Because it is a measure of the difference in spin population at the Fermi level, it is a measure of magnetization. Reversing the circular polarization direction (photon helicity) reverses the dichroism spectra.

Many groups, including ours, have been performing XMCD studies on oxide DMS materials for nearly ten years. None has observed a robust, transition metal (TM) XMCD signal that must exist if the TM atoms are magnetically ordered (pure cobalt shows an XMCD intensity of nearly twenty percent). In many instances a weak XMCD signal has been observed, but it could always be identified as a secondary phase, whether a ferromagnetic particulate (metal or oxide), or antiferromagnetic particulates with uncompensated spins, indicating these dichroism spectra are not associated with an intrinsic ferromagnetic semiconductor. Such has been the case for metal particulates in Co-doped TiO_2 [24].

In many cases the material synthesis can be refined to eliminate the secondary phase, still resulting in the same strong magnetic hysteresis behavior, but with an

undetectable XMCD signal. Because the magnetization curve is largely unaffected even though the XMCD signal is eliminated, the improved synthesis retains the ferromagnetic semiconductor properties while eliminating the ferromagnetic secondary phase responsible for the XMCD signal but not intrinsic to the magnetic semiconductor. It should be pointed out that the use of very high magnetic fields can also result in an unrelated XMCD signal, but this spectrum is not representative of the ferromagnetic semiconductor, and fields similar to those of the magnetization curves should always be used.

This null result is quite surprising because one of the most recent methods to study these materials, described by Neal et al. [25], uses low energy magnetic circular dichroism (visible MCD). The visible light dichroism is more difficult to decipher and does not possess the clear elemental resolution of the X-ray analogue, but it seems clearly related to the ferromagnetic semiconductor properties. It is a new tool to gain insight into the problem and is quickly becoming a mandatory measurement for any candidate oxide based ferromagnetic semiconductor. The visible MCD has been shown to occur in the same field range as the magnetization and can faithfully reproduce the hysteresis loops.

Why these materials exhibit a visible dichroism signal but no X-ray dichroism signal is an observation that has yet to be explained, and serves as a further restriction on any theoretical explanation. The most obvious explanation is that the visible MCD probes the magnetization of the charge carriers, whereas XMCD probes the magnetic character of the electronic structure of only a specific element with a localized core-hole. Visible MCD then seems an ideal identifier of carrier mediated ferromagnetism.

Our as-grown MOCVD synthesized samples also show no XMCD (see Figure 5) while maintaining a strong magnetization curve. Taking into account the results of the array of experiments conducted on our samples, we conclude that our as-grown cobalt doped TiO_2 samples are single phase DMS materials that are intrinsically ferromagnetic.

The origin of the ferromagnetism in DMS oxides is still somewhat of a mystery, with the Bound Magnetic Polaron (BMP) model currently the most widely accepted theory. First described by Kaminski and Das Sarma [26] and extended to the oxide based magnetic semiconductors by Coey [27], in some versions of the BMP model the long-range ferromagnetic order is established through interaction with the transition metal dopant's magnetic moment, implying that it must have a long-range ordering as well. The absence of any dichroism in the XMCD from DMS materials has prompted some to speculate that the origin of ferromagnetism is related to the concentration of oxygen vacancies [28,29]. However, this is inconsistent with our gas flow annealing studies (with and without the presence of oxygen in the annealing environment) of the $Co:TiO_2$ DMS materials. This suggests that the ferromagnetism is not due to oxygen vacancies, but is perhaps rather explained by crystalline defects [30].

IV. Conclusion

Liquid precursor MOCVD using TIP, $Co(TMHD)_3$, and THF combined in the manner previously described is a viable way to produce ferromagnetic $Ti_{1-x}Co_xO_2$ thin films in either the anatase or rutile structure. These films demonstrate room temperature ferromagnetism, and XAS and XMCD results indicate the true DMS nature of these

films. Interestingly, the ferromagnetic properties of the films vanish upon annealing in various atmospheres, suggesting the magnetism is not due to oxygen vacancies.

Acknowledgments

This research was supported by the Office of Naval Research under grant N00014-03-1-092.

The authors wish to thank Richard Smith for access to the Ion Beam Laboratory at Montana State University for the collection of Rutherford backscattering data.

The Advanced Light Source is supported by the Director, Office of Science, Office of Basic Energy Sciences, of the U.S. Department of Energy under Contract No. DE AC02-05CH11231.

References:

[1] G. A. Prinz, Science **282**, 1660 (1998).
[2] S. A. Wolf, Science **294**, 1488 (2001).
[3] Y. B. Xu, E. Ahmad, J. S. Claydon, et al., J. Magn. Magn. Mater. **304**, 69 (2006).
[4] Y. Matsumoto, M. Murakami, T. Shono, et al., Science **291**, 854 (2001).
[5] S. A. Chambers, C. M. Wang, S. Thevuthasan, , et al., Thin Solid Films **418**, 197 (2002).
[6] S. R. Shinde, S. B. Ogale, S. D. Sarma, et al., Phys. Rev. B **67**, 115211 (2003).
[7] J. W. Quilty, A. Shibata, J.-Y. Son, et al., Phys. Rev. Lett. **96**, 027202 (2006).
[8] S. J. Pearton, C. R. Abernathy, M. E. Overberg, et al., J. of Appl. Phys. – Appl. Phys. Rev. **93**, 1 (2003).
[9] K. R. Kittilstved, D. A. Schwartz, A. C. Tuan, S. M. Heald, S. A. Chambers, and D. R. Gamelin, Phys. Rev. Lett. **97**, 037203 (2006).
[10] N. M. Sbrockey, J. D. Cuchiaro, B. H. Hoerman, L. G. Provost, C. E. Rice, S. Sun, and G. S. Tompa, Vac. Tech. and Coating, May, 44 (2004).
[11] N.-J. Seong, S.-G. Yoon, and C.-R. Cho, Appl. Phys. Lett. **81**, 4209 (2002).
[12] R. Brydson, H. Sauer, W. Engel, et al., J. Phys.:Condens. Matter **1**, 797 (1989).
[13] F. M. F. de Groot, J. C. Fuggle, B. T. Thole, and G. A. Sawatzky, Phys. Rev. B **41**, 928 (1990)
[14] F. M. F. de Groot, et al., Phys. Chem. Minerals **19**, 140 (1992).
[15] A. Lussier, J. Dvorak, Y. U. Idzerda, et al., Physica Scripta **T115**, 623 (2005).
[16] S. A. Chambers, S. Thevuthasan, R. F. C. Farrow, et al., Appl. Phys. Lett. **79**, 3467 (2001).
[17] Y. Xin, K. Han, P. A. Stampe, and R. J. Kennedy, J. Crystal Growth **290**, 459 (2006).
[18] M. G. Samant, J. Stohr, S. S. P. Parkin, et al., Phys. Rev. Lett. **72**, 1112 (1994).
[19] V. Chakarian, Y. U. Idzerda, C.-C. Kao, and C. T. Chen, J. Magn. Magn. Mater. **165**, 52 (1997).
[20] C. T. Chen, Y. U. Idzerda, H.-J. Lin, et al., Phys. Rev. B **48**, 642 (1993).
[21] B. T. Thole, P. Carra, F. Sette, and G. van der Laan, Phys. Rev. Lett. **68**, 1943 (1992).
[22] P. Carra, B. T. Thole, M. Altarelli, and X. Wang, Phys. Rev. Lett. **70**, 694 (1993).
[23] C. T. Chen, Y. U. Idzerda, H.-J. Lin, et al., Phys. Rev. Lett. **75**, 152 (1995).
[24] J.-Y. Kim, J.-H. Park, B.-G. Park, et al., Phys. Rev. Lett. **90**, 017401 (2003).
[25] J. R. Neal, A. J. Behan, R. M. Ibrahim, et al., Phys. Rev. Lett. **96**, 197208 (2006).
[26] A. Kaminski, S. Das Sarma, Phys. Rev. Lett. **88**, 247202 (2002).
[27] J. M. D. Coey, M. Venkatesan, and C. B. Fitzgerald, Nature Materials **4**, 173 (2005).
[28] J. M. D. Coey, M. Venkatesan, P. Stamenov, C. B. Fitzgerald, and L. S. Dorneles, Phys. Rev. B **72**, 024450 (2005).
[29] J. Osorio-Guillen, S. Lany, S. V. Barabash, and A. Zunger, Phys. Rev. Lett. **96**, 107203 (2006).
[30] T. C. Kaspar, S. M. Heald, C. M. Wang, et al., Phys. Rev. Lett. **95**, 217203 (2005).

Figures:

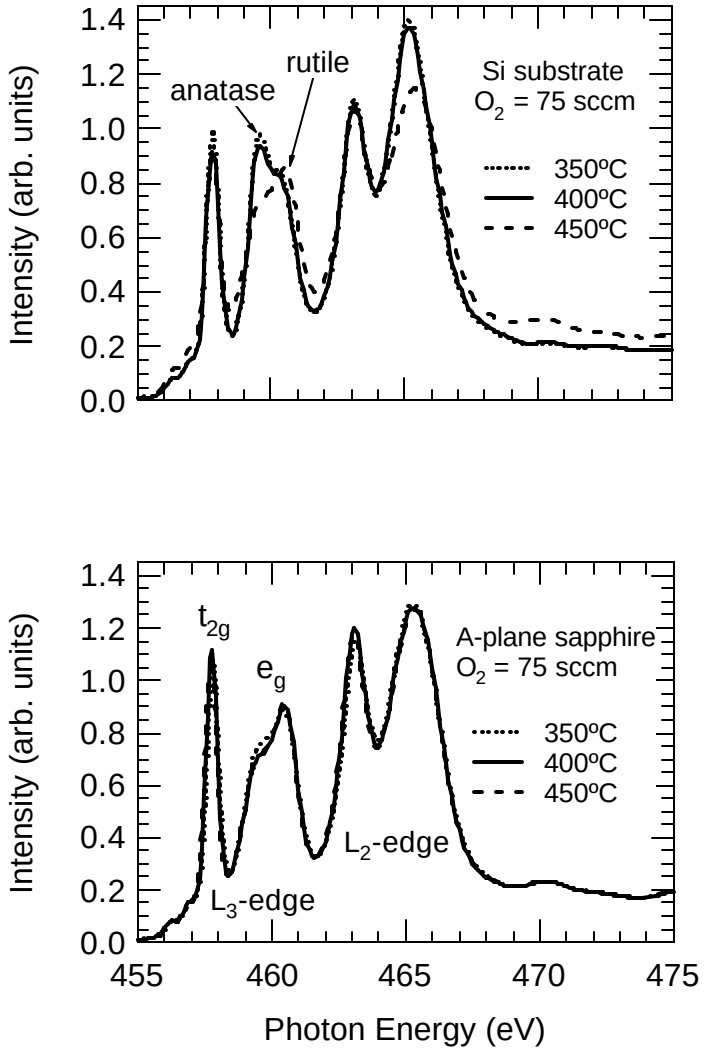

Figure 1: Ti $L_{2,3}$-edge XAS spectra of Co:TiO_2 thin films deposited by MOCVD at various temperatures on SiO_2/Si and A-plane Al_2O_3.

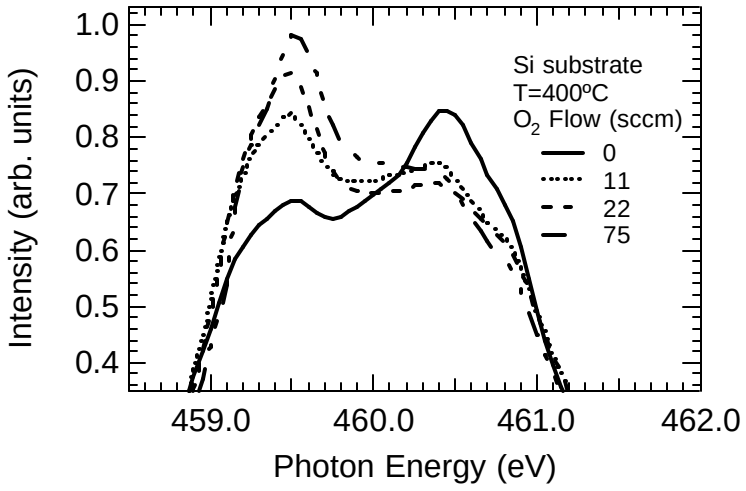

Figure 2: Ti edge XAS spectra demonstrating the effect of O_2 flow-rate on the TiO_2 phase. (He = 45 sccm)

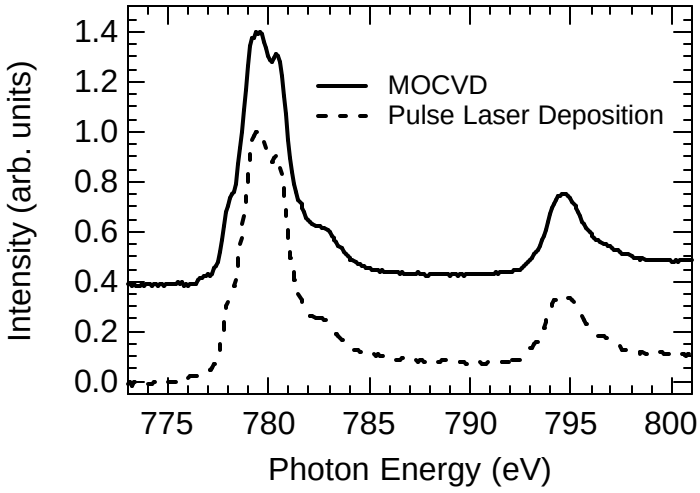

Figure 3: Comparison Co $L_{2,3}$-edge XAS; the cobalt incorporates at the Ti sites.

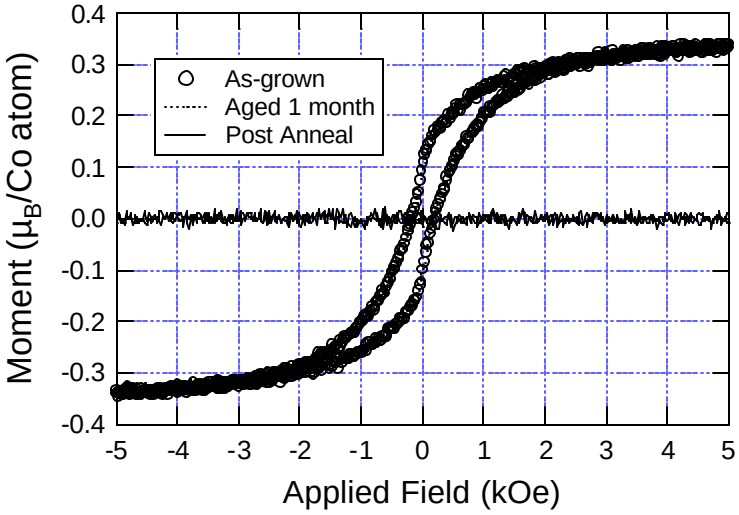

Figure 4: Representative VSM data from MOCVD deposited Co:TiO_2 thin films.

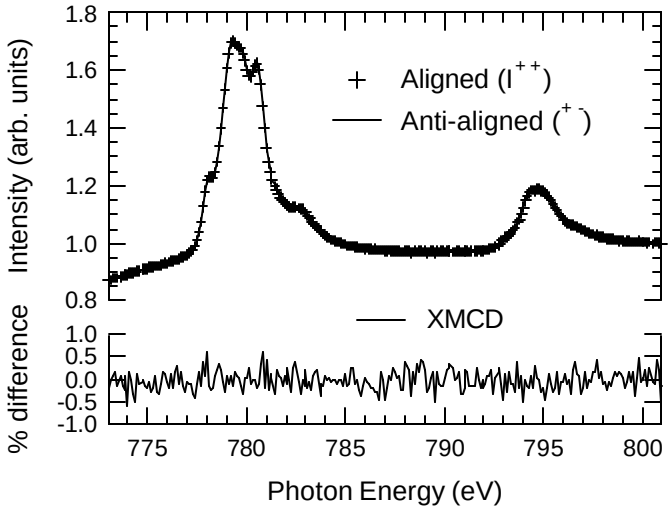

Figure 5: XMCD spectra of the Co $L_{2,3}$-edge. The intensity is proportional to the absorption cross section of right (+) and left (-) circularly polarized light.